Spectroscopic and crystal field studies of $YAlO_3$ single crystals doped with Mn ions

2009 J. Phys.: Condens. Matter 21 025404

(http://iopscience.iop.org/0953-8984/21/2/025404)

J. Phys.: Condens. Matter **21** (2009) 025404 (5pp) doi:10.1088/0953-8984/21/2/025404

Spectroscopic and crystal field studies of $YAlO_3$ single crystals doped with Mn ions

M G Brik[1,3], I Sildos[1], M Berkowski[2] and A Suchocki[2]

[1] Institute of Physics, University of Tartu, Riia 142, Tartu 51014, Estonia
[2] Institute of Physics, Polish Academy of Sciences, 32/46 Aleja Lotników, 02-668 Warsaw, Poland

E-mail: brik@fi.tartu.ee

Received 9 October 2008, in final form 2 November 2008
Published 11 December 2008
Online at stacks.iop.org/JPhysCM/21/025404

Abstract

Detailed analysis of the spectroscopic properties of the $YAlO_3$ crystals doped with manganese ions has been performed. The exchange charge model of the crystal field was used to calculate the crystal field parameters and energy levels of the Mn^{4+} and Mn^{5+} ions in $YAlO_3$. It was shown that both ions contribute to the formation of the absorption spectra. The calculated energy levels are in good agreement with the main observed absorption peaks. Comparison of the Racah parameters B for both ions in $YAlO_3$ with those for free ions shows a significant role played by the covalent effects, especially for Mn^{5+}.

(Some figures in this article are in colour only in the electronic version)

1. Introduction

Crystals doped with transition metal ions with unfilled 3d electron shells attract considerable interest of researchers due to their numerous applications in various optical devices. Among these ions, those having the $3d^2$ and $3d^3$ electron configurations are of particular interest, since they can produce either broad luminescence bands (which correspond to the $^3T_2 \rightarrow {}^3A_2$ ($3d^2$) or $^4T_{2g} \rightarrow {}^4A_{2g}$ ($3d^3$) spin-allowed transitions) or very sharp emission lines (corresponding to the $^1E \rightarrow {}^3A_2$ ($3d^2$) or $^2E_g \rightarrow {}^4A_{2g}$ ($3d^3$) spin-forbidden transitions). The former situation can be realized in weak or medium crystal fields, whereas the latter is an unambiguous manifestation of the strong crystal field around an impurity ion. The nature and character of the impurity ion emission is determined by a complicated interplay of several factors such as the charge of the ligands and impurity ions, coordination number of the impurity ion, applied pressure, interionic distance etc.

The most studied $3d^3$ ion is Cr^{3+}, which was the first ion (in Al_2O_3) used in the first laser [1]. After that pioneering work, many other crystals doped with Cr^{3+} were studied [2]. Another $3d^3$ ion is Mn^{4+}, also widely studied [3–5]. Among the Mn-doped materials, the yttrium aluminum perovskite $YAlO_3$ (YAP) is known to be a suitable host for solid-state lasers [6] and optical data storage [7, 8], and a material for thermoluminescence dosimetry of γ-radiation [9]. However, it should be pointed out that the Mn^{4+} ions are not stable and are subject to the $Mn^{4+} \rightarrow Mn^{5+}$ photoionization [10, 11], which leads to change of color of as-grown $YAlO_3$:Mn from yellowish to grayish or bluish. So, both Mn^{4+} and Mn^{5+} ions are present in the YAP crystal and reveal themselves in the absorption spectrum.

The main aim of the present paper is to perform detailed consideration of the experimental absorption spectra of the YAP:Mn crystals supplied with consistent crystal field analysis (starting from the structural data) of the Mn^{4+} and Mn^{5+} energy levels in the considered host, which, to the best of our knowledge, is lacking in the literature.

2. Crystal growth and experimental spectroscopic details

YAP is an orthorhombic crystal, space group $Pnma$, space group number 62 [12]. Lattice constants (in Å) are $a = 5.330$, $b = 7.375$, $c = 5.180$; one unit cell contains four formula units. Al ions are sixfold coordinated by oxygen ions, and Y ions 12-fold coordinated. After doping, Mn ions substitute for Al ions, entering positions of distorted octahedral symmetry. Figure 1 shows one unit cell of YAP; it can be described as oxygen octahedral chains along the b axis.

[3] Author to whom any correspondence should be addressed.

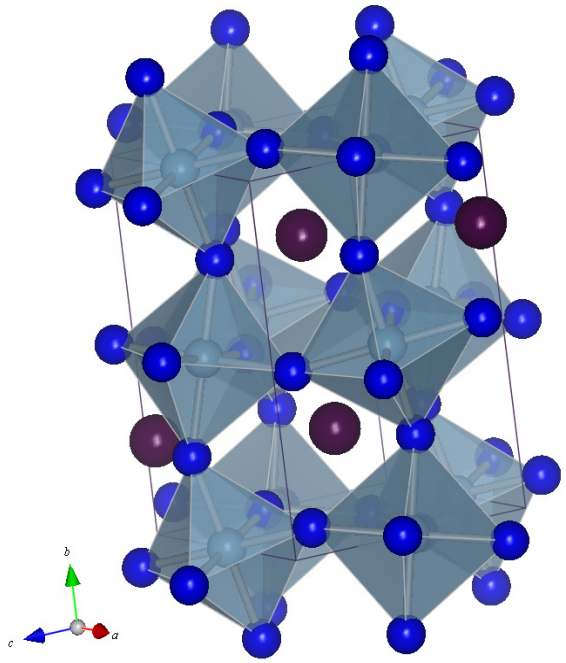

Figure 1. One unit cell of $YAlO_3$. Coordination polyhedra around Al ions are shown. Y ions are shown by black spheres. Drawn with VICS-II, developed by Izumi and Dilanian.

More recent studies have shown that the crystallographic structure of these crystals can be described in the *Pbnm* space group coordinates with lattice parameters (in Å) $a = 5.179\,01(7)$, $b = 5.326\,63(7)$, $c = 7.369\,71(9)$; $Z = 4$. The unconventional space group *Pbnm* was adopted instead of *Pnma* because most of the isotypical compounds had been described in this setting. The conversion to the standardized space group *Pnma* can be provided by a conversion matrix $\begin{pmatrix} 0 & 1 & 0 \\ 0 & 0 & 1 \\ 1 & 0 & 0 \end{pmatrix}$ [13].

Since the electrical charges of the substituted Al^{3+} and substituting Mn^{4+} ions are different, the charge compensating mechanisms should be arranged to maintain electric neutrality of the samples. As was suggested in [14], Mn^{2+} and Mn^{4+} ions can serve as the charge compensators, entering the Y^{3+} and Al^{3+} positions, respectively. Additionally, the cation vacancies can also play the role of charge compensating defects.

Single crystals of $YAlO_3$ doped with manganese were grown by the Czochralski method in the Institute of Physics, Polish Academy of Sciences. The crystals were grown in a pure nitrogen atmosphere from the melt containing 4 mol% more yttrium than aluminum oxide in comparison with the stoichiometric composition. The manganese concentration in the studied $YAlO_3$:Mn crystal corresponds to 0.2% in the melt with respect to aluminum content. The 'as grown' crystals were slightly bluish, which is a fingerprint of the presence of some Mn^{5+} ions in addition to the Mn^{4+} ions usually detected in those crystals. Illumination with an argon ion or another visible laser photo-transforms some Mn^{4+} to the Mn^{5+} ions, which makes the crystal more bluish or even grayish.

The optical absorption spectra were measured with a Cary 5000 UV–vis–NIR spectrophotometer at room temperature.

3. Crystal field calculations and comparison with experimental data

We have used the exchange charge model (ECM) of the crystal field [15] for calculations of the energy levels of the Mn ions in the YAP crystal. One of the main advantages of the ECM is that there is no need to impose any restrictions on the symmetry of an impurity center. The parameters of the crystal field acting upon an impurity ion can be calculated directly from the structural data for a particular host available in the literature.

In the ECM framework, the energy levels of a 3d ion in a crystal field (CF) of arbitrary symmetry are represented by the eigenvalues of the following CF Hamiltonian [15]:

$$H_{\mathrm{CF}} = \sum_{p=2,4} \sum_{k=-p}^{p} B_p^k O_p^k, \tag{1}$$

where O_p^k are suitable linear combinations of the irreducible tensor operators acting on the angular parts of the impurity ion wavefunctions and B_p^k are the crystal field parameters (CFPs), which contain all information about the symmetry of an impurity center and interactions between an impurity ion and ligands. Decreasing the symmetry of a considered cluster leads to an increase of the number of non-zero CFPs and more complicated form of the CF Hamiltonian. The CFPs in the ECM approach are written as a sum of two terms:

$$B_p^k = B_{p,q}^k + B_{p,S}^k, \tag{2}$$

where the first term

$$B_{p,q}^k = -K_p^k e^2 \langle r^p \rangle \sum_i q_i \frac{V_p^k(\theta_i, \varphi_i)}{R_i^{p+1}} \tag{3}$$

describes the electrostatic interaction between the central ion and the ith lattice ions with electrical charges q_i and spherical coordinates R_i, θ_i, φ_i. The $V_p^k(\theta, \varphi)$ polynomials, the K_p^k, γ_p numerical factors and the O_p^k operators are defined in [15]. The $\langle r^p \rangle$ entries are the mean values of the radial coordinates of the d electrons of a given impurity ion, which can be easily calculated numerically or taken from the literature [16]. The second term of equation (2) is proportional to the overlap between the wavefunctions of the central ion and the ligands. Inclusion of this term allows for an effective modeling of the covalent effects which change electron density in the space between an impurity ion and ligands. It can be calculated as follows:

$$B_{p,S}^k = K_p^k e^2 \frac{2(2p+1)}{5} \sum_i (G_s S(s)_i^2 + G_\sigma S(\sigma)_i^2 + \gamma_p G_\pi S(\pi)_i^2) \frac{V_p^k(\theta_i, \varphi_i)}{R_i}. \tag{4}$$

Here $S(s)$, $S(\sigma)$ and $S(\pi)$ correspond to the overlap integrals between the d functions of the central ion and the p and s functions of the ligands: $S(s) = \langle d0|s0\rangle$, $S(\sigma) = \langle d0|p0\rangle$, $S(\pi) = \langle d1|p1\rangle$. G_s, G_σ and G_π are dimensionless adjustable parameters of the model, whose values can be determined from the positions of the first three absorption bands. Usually, they can be approximated to a single value,

Table 1. Crystal field and Racah parameters (in cm^{-1}) in Stevens normalization for Mn^{4+} and Mn^{5+} in $YAlO_3$. The calculated averaged values (in au) of $\langle r^2\rangle$ and $\langle r^4\rangle$ are also given.

	Mn^{4+}	Mn^{5+}
B_2^{-2}	895	716
B_2^{-1}	668	804
B_2^0	369	290
B_2^1	−1831	−1563
B_2^2	−300	−243
B_4^{-4}	−16 616	−9258
B_4^{-3}	−147 22	−8332
B_4^{-2}	1440	802
B_4^{-1}	−5861	−3261
B_4^0	4039	2260
B_4^1	−22 963	−127 89
B_4^2	2640	1471
B_4^3	−23 504	−13 092
B_4^4	−19 493	−10 908
G (exchange charge model parameter)	6.17	8.51
B	720	485
C	3025	2256
$\langle r^2\rangle$	1.098 76	0.968 05
$\langle r^4\rangle$	2.402 00	1.790 97

i.e. $G_s = G_\sigma = G_\pi = G$, thus reducing the number of fitting parameters to one only, which can be determined from the position of the lowest (in energy) absorption band. This is usually a reasonable approximation [15].

When calculating the electrostatic contribution to the CFPs (equation (3)), special attention should be paid to the convergence of the involved crystal lattice sums, especially for the second rank parameters $p = 2$. To ensure proper convergence, we have considered a large cluster around the Mn ion consisting of 20 620 ions, thus including the contributions from the ions located at the distances up to 52 Å from the central ion. Since both Mn^{4+} and Mn^{5+} ions contribute to the absorption spectra, the CF calculations were carried out for each case separately. The Mn^{4+}–O^{2-} and Mn^{5+}–O^{2-} overlap integrals needed for the proper application of the ECM were calculated numerically using the radial parts of these ions' wavefunctions given in [17, 18] and approximated then by the following exponential functions of the Mn–O distance r:

$$S_s = \langle d0|s0\rangle = -0.823\,03\exp(-0.829\,05r), \quad (5)$$

$$S_\sigma = \langle d0|p0\rangle = 0.703\,70\ \exp(-0.741\,30r), \quad (6)$$

$$S_\pi = \langle d1|p1\rangle = 1.495\,70\ \exp(-1.105\,40r) \quad (7)$$

for the Mn^{5+}–O^{2-} overlap integrals, and

$$S_s = \langle d0|s0\rangle = -0.921\,25\exp(-0.698\,07r), \quad (8)$$

$$S_\sigma = \langle d0|p0\rangle = 0.851\,14\exp(-0.741\,51r), \quad (9)$$

$$S_\pi = \langle d1|p1\rangle = 1.464\,40\exp(-1.102\,30r) \quad (10)$$

for the Mn^{4+}–O^{2-} overlap integrals.

Table 2. Calculated energy levels (in cm^{-1}) of Mn^{4+} ions in $YAlO_3$.

		Observed	
Energy levels	Calc.	Reference [14]	This work, figure 2
$^4A_2$	0	0	
^2E	14 410	13 996	14 436
	14 460		14 465
$^2T_1$	15 040		
	15 050		
	15 090		
$^4T_2$	20 682	20 833	21 000
	21 040		
	21 300		
$^2T_2$	22 180		
	22 200		
	22 370		
$^4T_1$ (^4F)	27 710	26 300–31 250	
	28 720		
	29 120		

Table 3. Calculated energy levels (in cm^{-1}) of Mn^{5+} ions in $YAlO_3$.

Energy levels	Calc.	Observed
$^3T_1$ (^3F)	0	
	450	
	670	
^1E	7 650	7800–8500
	7 740	
$^1T_2$	8 210	
	8 370	
	8 530	
$^3T_2$	10 990	11 000
	11 120	
	11 370	
$^3T_1$ (^3P)	17 060	18 000
	17 300	
	18 230	
$^1A_1$	16 750	
$^1T_2$	19 580	
	19 680	
	19 950	
$^1T_1$	21 130	
	21 370	
	22 270	
$^3A_2$	22 930	

Table 1 lists the values of the CFPs calculated with equations (3)–(10) and structural data from [12].

The CFP values from the above table were used to diagonalize the CF Hamiltonian for Mn^{4+} and Mn^{5+} ions in the space spanned by all LS wavefunctions of their corresponding electron configurations (25 wavefunctions of the ^3F, ^3P, ^1S, ^1D, ^1G terms of Mn^{5+} and 50 wavefunctions of the ^4F, ^4P, ^2P, $^2D_1$, $^2D_2$, ^2F, ^2G, ^2H terms of Mn^{4+}). Spin–orbit interaction was neglected, since the absorption bands are broad, and their fine structure can hardly be resolved. Tables 2 and 3 summarize the results of these calculations. The relative error of the energy level calculations is basically determined by the accuracy of the ionic positions in a unit cell and is not expected to be greater than 0.5–1%.

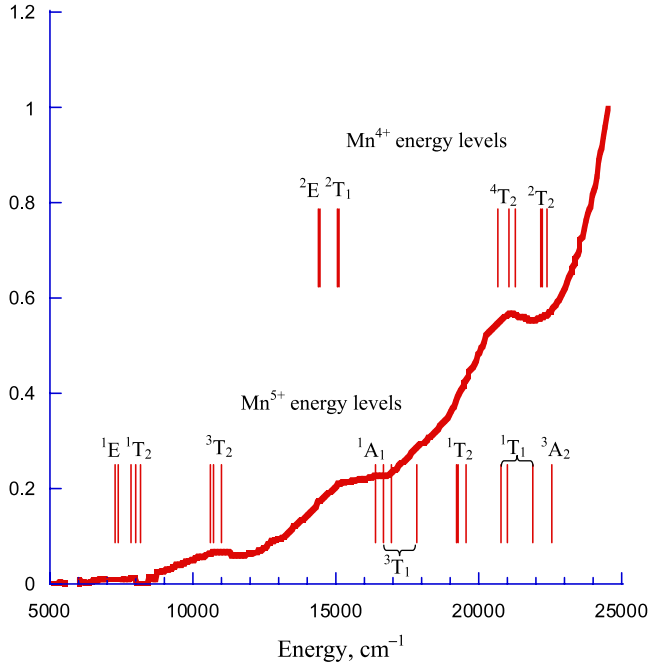

Figure 2. Comparison between the experimental [6] absorption spectrum of $YAlO_3$:Mn and calculated (this work) Mn^{5+} and Mn^{4+} energy levels. The Mn^{5+} energy levels were shifted to the lower energies by 374 cm^{-1} (which corresponds to the barycenter of the ground $^3T_1$ state).

Finally, figure 2 represents the correspondence between the experimental absorption spectrum and the calculated energy levels of the manganese ions (shown as the vertical lines).

As seen from the figure, the YAP:Mn absorption spectrum cannot be attributed to the Mn^{4+} ions only, but should be analyzed as a superposition of the two absorption spectra originating from the Mn^{4+} and Mn^{5+} ions. A wide absorption band at about 21 000 cm^{-1} is caused by the $^4A_2 \rightarrow {}^4T_2$ (^{4}F) absorption transition of Mn^{4+} ions. Another wide absorption band from about 14 000 to 18 000 cm^{-1} has a complicated origin and is due to the spin-allowed $^3T_1(^3F) \rightarrow {}^3T_1(^3P)$ transition of Mn^{5+} with admixture of the spin-forbidden $^3T_1(^3F) \rightarrow {}^1A_1$ transition of Mn^{5+} and $^4A_2 \rightarrow {}^2E$, $^2T_1$ transitions of Mn^{4+} ions. All these transitions are broadened by the electron–vibrational interaction. A weak absorption at about 7800–8500 cm^{-1} is caused by the $^3T_1(^3F) \rightarrow {}^1E$, $^1T_2$ transitions of Mn^{5+} ions. A very broad and intensive absorption band at about 26 000 cm^{-1} is due to a certain unidentified intrinsic defect of the YAP crystals [14], most probably associated with the oxygen vacancies, onto which the spin-allowed transition $^4A_2 \rightarrow {}^4T_1$ (^{4}F) of Mn^{4+} is superimposed [19].

Since the lowest excited states for both Mn^{4+} and Mn^{5+} states have a multiplicity different from that for the ground state, both impurity centers can be characterized by strong CF, which can be confirmed by the high Dq/B ratios (about 2.3 for Mn^{5+} and 2.9 for Mn^{4+}, which locate both ions in the 'strong field part' of the corresponding Tanabe–Sugano diagrams). It is also worthwhile to note that the values of the Racah parameter B for both ions are significantly reduced in comparison with those for free ions. The nephelauxetic ratios $\beta = B_{\text{crystal}}/B_{\text{free ion}}$ are equal to 0.396 for Mn^{5+} and 0.621 for Mn^{4+} ($B_{\text{free ion}} = 1224$ cm^{-1} for Mn^{5+} [20] and 1160 cm^{-1} for Mn^{4+}) [21]. Such a significant reduction of the Racah parameters indicates an essential role played by the covalent effects in the formation of the optical properties of the YAP:Mn crystals; these effects are more pronounced in the case of the Mn^{5+} ions.

The CF calculations of the energy levels of Mn ions in $YAlO_3$ presented here constitute a further improvement of the previously published [10, 14] analysis based on the cubic CF approximation. In this connection, it is worthwhile to point out here that no *a priori* symmetry assumptions were used in our calculations. Instead, starting from the crystal structure data we have performed consistent CF calculations which allowed for explicit treatment of the low symmetry components of CF and estimation of the low symmetry splitting of the orbital triplet states (which was not considered in the above cited publications).

It should be also emphasized that the charge compensating effects (like the cation vacancies or presence of the manganese ions in other oxidation states) also affect the optical properties of the YAP:Mn crystal [19]. These defects can also distort the crystal environment around impurity centers. Since the distribution of these defects cannot be determined and thus cannot be effectively modeled in the CFP calculations, we assume that they produce inhomogeneous broadening of the absorption lines, which can be seen in asymmetric shapes of the main absorption bands.

4. Conclusions

A detailed study of the $YAlO_3$:Mn crystal (starting with the crystal growth and ending up with the crystal field calculations and absorption band assignment) has been performed in the present paper. The exchange charge model of crystal field has been used for the first time to calculate the crystal field parameters and describe the energy level schemes of the manganese ions in the studied host. The results of the crystal field analysis confirm the presence of the manganese ions in at least two oxidation states in $YAlO_3$ (as Mn^{4+} and Mn^{5+}). It should be emphasized that only one fitting parameter of the exchange charge model of the crystal field was allowed to vary freely. Nevertheless, the positions of the main absorption bands determining the overall appearance of the absorption spectrum are in good agreement with the calculated energy levels.

Acknowledgment

This work was partially supported by a grant from the Polish Ministry of Science and Education for the years 2006–2009.

References

[1] Maiman T H 1960 *Nature* **187** 493
[2] Kück S 2001 *Appl. Phys.* B **72** 515 and references therein
[3] Geschwind S, Kisliuk P, Klein M P, Remeika J P and Wood D L 1962 *Phys. Rev.* **126** 1684

[4] Petermann K and Huber G 1984 *J. Lumin.* **31/32** 71
[5] Brenier A, Suchocki A, Pedrini C, Boulon G and Madej C 1992 *Phys. Rev.* B **46** 3219
[6] Zhydachevskii Ya, Galanciak D, Kobyakov S, Berkowski M, Kaminska A, Suchocki A, Zakharko Ya and Durygin A 2006 *J. Phys.: Condens. Matter* **18** 11385
[7] Loutts G B, Warren M, Taylor L, Rakhimov R R, Ries H R, Miller G, Noginov M A, Curley M, Noginova N, Kukhtarev N, Caulfield H J and Venkateswarlu P 1998 *Phys. Rev.* B **57** 3706
[8] Noginov M A, Noginova N, Curley M, Kukhtarev N, Caulfield H J, Venkateswarlu P and Loutts G B 1998 *J. Opt. Soc. Am.* B **15** 1463
[9] Zhydachevskii Ya, Durygin A, Suchocki A, Matkovskii A, Sugak D, Bilski P and Warchol S 2005 *Nucl. Instrum. Methods* B **227** 545
[10] Noginov M A, Loutts G B, Noginova N, Hurling S and Kück S 2000 *Phys. Rev.* B **61** 1884
[11] Zhydachevskii Ya, Suchocki A, Sugak D, Luchechko A, Berkowski M, Warchol S and Jakieła R 2006 *J. Phys.: Condens. Matter* **18** 5389
[12] Diehl R and Brandt G 1975 *Mater. Res. Bull.* **10** 85
[13] Vasylechko L, Matkovskii A, Savytskii D, Suchocki A and Vallrafen F 1999 *J. Alloys Compounds* **291** 57
[14] Noginov M A and Loutts G B 1999 *J. Opt. Soc. Am.* B **16** 3
[15] Malkin B Z 1987 Crystal field and electron–phonon interaction in rare-earth ionic paramagnets *Spectroscopy of Solids Containing Rare-Earth Ions* ed A A Kaplyanskii and B M Macfarlane (Amsterdam: North-Holland) pp 33–50
[16] Abragam A G and Bleaney B 1970 *Electron Paramagnetic Resonance of Transition Ions* (Oxford: Clarendon) chapter 7
[17] Clementi E and Roetti C 1974 *At. Data Nucl. Data Tables* **14** 177
[18] Eremin M V 1989 *Spectroscopy of Laser Crystals* ed A A Kaplyanskii (Leningrad: Nauka) p 30 (in Russian)
[19] Zhydachevskii Ya, Durygin A, Suchocki A, Matkovskii A, Sugak D, Loutts G B and Noginov M A 2004 *J. Lumin.* **109** 39
[20] Capobianco J A, Cormier G, Morrison C A and Moncorgé R 1992 *Opt. Mater.* **1** 209
[21] Uylings P H M, Raassen A J J and Wyart J F 1984 *J. Phys. B: At. Mol. Phys.* **17** 4103